PHYSICAL REVIEW E, VOLUME 64, 015201(R)

Noise-resistant chaotic synchronization

T. L. Carroll
U.S. Naval Research Laboratory, Washington, DC 20375
(Received 1 November 2000; published 18 June 2001)

The practical applications of self-synchronizing chaotic systems are greatly limited by their sensitivity to noise. Even small amounts of noise added to the synchronizing signal can degrade synchronization to the point where information encoded on the chaotic signal can't be recovered. In this paper, I show that it is possible to build chaotic circuits that operate on two different time scales. The separation of time scales allows the low frequency part of the circuit to average out noise added to the synchronizing signal. Adjusting the relative time scales of the two parts of the circuit allow one to make the synchronization error arbitrarily close to the error caused by circuit mismatch for any amount of added noise.

DOI: 10.1103/PhysRevE.64.015201 PACS number(s): 05.45.Gg, 05.45.Vx, 05.45.Xt

INTRODUCTION

While chaotic synchronization has been proposed as a method of spread spectrum communication [1–11], self-synchronizing chaotic systems suffer from a problem common to all self-synchronizing communication systems: since the synchronizing signal is also the carrier signal, any noise present during transmission contaminates the synchronizing signal and degrades synchronization [12]. The problem is made worse by the fact that chaotic systems are nonlinear, so the noise becomes mixed with the chaotic carrier signal in a nonlinear fashion, making separation of signal from noise by conventional means impossible. There are noise reduction techniques for chaotic signals [13–17], but they either work only when the noise is less than 10% of the signal or they require much computation.

The circuit described in this paper reduces the noise added to the synchronizing signal by averaging the chaotic signal over a long time scale. The circuit actually has dynamics at two distinct time scales. The synchronizing signal drives the faster of the two time scales while the slower time scale acts to average out the noise.

THE CIRCUIT

It is possible to synchronize a chaotic system after the synchronizing signal has been filtered; one passes the identical signal from the response system through an identical filter, and then uses the difference between filtered signals to synchronize the response system [18,19]. While this method can filter out some noise, filtering the response signal lessens the stability of the synchronized response system, so maintaining synchronization may be difficult.

Rulkov and Tsimring built filters into a chaotic circuit to overcome this stability problem [20], but in their work, they were interested in limiting the bandwidth of the chaotic synchronization, not in reducing noise.

The basic idea behind this circuit was suggested by experimental work involving ferromagnetic resonance in yttrium iron garnet [21–24]. When driven with the proper microwave signal, a sample of yttrium iron garnet displays dynamics at two different time scales. The driving signal is in the gigahertz range, but the yttrium iron garnet may display chaotic dynamics in the kilohertz range. If a circuit with two different time scales was constructed, then noise contaminating the high frequency signals might be averaged out in the low frequency part of the circuit.

Such a circuit has been built. This circuit is based on coupling together two piecewise linear Rossler circuits [25] with different frequencies. Mathematically, the circuit may be described by

$$\frac{dx_1}{dt} = -\frac{1}{RC_1}(\gamma_1 x_1 + 0.5x_2 + x_3 + 0.5|x_4|), \tag{1a}$$

$$\frac{dx_2}{dt} = -\frac{1}{RC_1}(-x_1 + \gamma_2 x_2 + x_6), \tag{1b}$$

$$\frac{dx_3}{dt} = -\frac{1}{RC_1}(-g(x_1) + x_3), \tag{1c}$$

$$\frac{dx_4}{dt} = -\frac{1}{RC_2}(x_1 + 0.05x_4 + 0.5x_5 + x_6), \tag{1d}$$

$$\frac{dx_5}{dt} = -\frac{1}{RC_2}(-x_4 + 0.11x_5), \tag{1e}$$

$$\frac{dx_6}{dt} = -\frac{1}{RC_2}(-g(x_4) + x_6), \tag{1f}$$

$$g(x) = \left\{ \begin{array}{ll} 0 & x<3 \\ 15(x-3) & x\geqslant 3 \end{array} \right\}, \tag{1g}$$

where γ_1 and γ_2 may be varied, $R = 10^5\,\Omega$, and C_1 and C_2 may be varied to alter the relative time scales of the two parts of the circuit. The signals x_1 through x_3 form the low frequency part of the circuit, while x_4 through x_6 form the high frequency part.

Figure 1 shows different projections of the attractor for the circuit when $C_1 = 0.01$ μF, $C_2 = 0.001$ μF, $\gamma_1 = 0.05$, and $\gamma_2 = 0.02$, so that the time scales are separated by a factor of 10. Figure 1(a) is a plot of x_2 versus x_1 , while Fig. 1(b) shows x_5 versus x_4. Figure 2 shows power spectra of two different signals from the circuit. Figure 2(a) shows the power spectrum of x_1, while Fig. 2(b) shows the power spec-

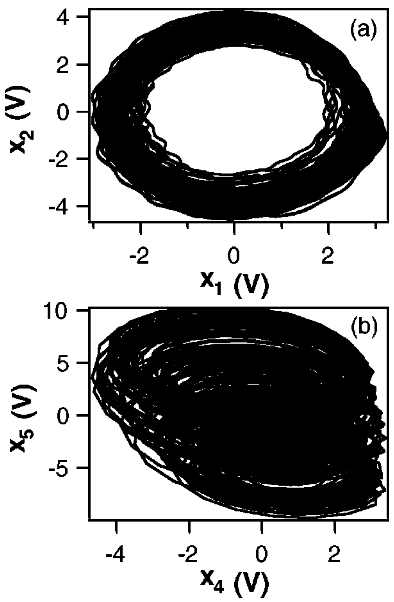

FIG. 1. Two projections of the attractor for the circuit described by Eq. (1) when $C_1=0.01$ μF and $C_2=0.001$ μF (data from the circuit). (a) x_2 vs x_1 (lower frequency part) (b) x_5 vs x_4 (higher frequency part).

trum of x_4. The higher frequency peak in the power spectrum, most prominent in Fig. 2(b), is at 1110 Hz. The lower frequency peak in the power spectrum, largest in Fig. 2(a), is at 111 Hz.

Choosing different capacitors altered the relative frequencies of the main peaks in the power spectrum of the circuit. Setting $C_1=0.1$ μF, $C_2=0.001$ μF, $\gamma_1=0.02$, and $\gamma_2=0.02$ resulted in the power spectra seen in Fig. 3. Figure 3(a) is the power spectrum of x_1, and 3(b) is the power spectrum of x_4. The peak frequency in x_4 is still at 1110 Hz, but the peak frequency in x1 is now at 11.1 Hz.

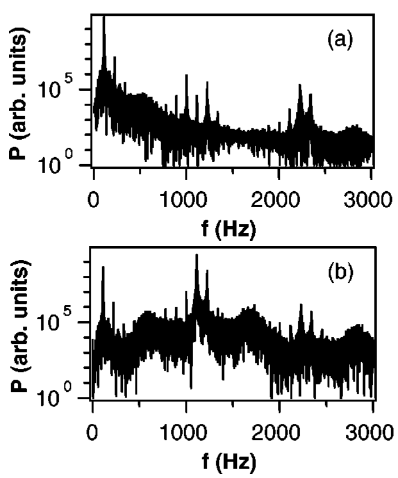

FIG. 2. (a) Power spectrum P for the x_1 signal from the circuit when $C_1=0.01$ μF and $C_2=0.001$ μF. (b) Power spectrum P for the x_4 signal from the circuit when $C_1=0.01$ μF and $C_2=0.001$ μF.

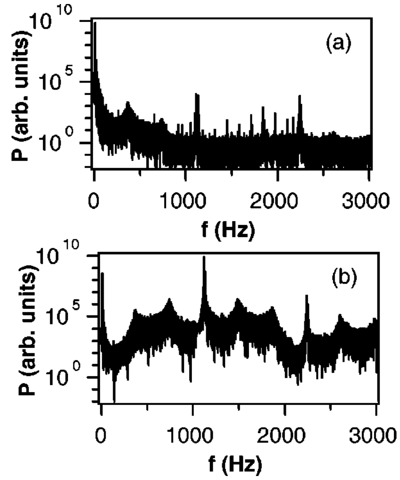

FIG. 3. (a) Power spectrum P for the x_1 signal from the circuit when $C_1=0.1$ μF and $C_2=0.001$ μF. (b) Power spectrum P for the x_4 signal from the circuit when $C_1=0.1$ μF and $C_2=0.001$ μF.

SYNCHRONIZATION

A second circuit was built that closely matched the drive circuit described by Eq. (1). A linear combination of signals from the drive circuit was used to synchronize the response circuit. The response system was described by

$$x_t=\sum_{i=1}^{6} k_i x_i^d, \quad x_r=\sum_{i=1}^{6} k_i x_i^r, \tag{2a}$$

$$\frac{dx_1^r}{dt}=-\frac{1}{RC_1}(\gamma_1 x_1^r+0.5x_2^r+x_3^r+0.5|x_4^r|), \tag{2b}$$

$$\frac{dx_2^r}{dt}=-\frac{1}{RC_1}(-x_1^r+\gamma_2 x_2^r+x_6^r), \tag{2c}$$

$$\frac{dx_3^r}{dt}=-\frac{1}{RC_1}[-g(x_1^r)+x_3^r], \tag{2d}$$

$$\frac{dx_4^r}{dt}=-\frac{1}{RC_2}[x_1^r+0.05x_4^r+0.5x_5^r+x_6^r+b_4(x_t-x_r)], \tag{2e}$$

TABLE I. k and b parameters used to synchronize the response circuit.

i	k_i	b_i
1	-4.59	0
2	5.61	0
3	3.16	0
4	-0.79	1.11
5	-0.21	-0.38
6	0.36	0.33

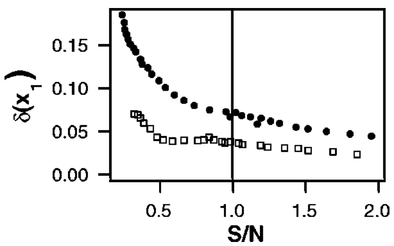

FIG. 4. rms synchronization error $\delta(x_1)$ from the circuit as a function of rms signal to noise ratio S/N. The dark circles correspond to $C_1=0.01$ μF and $C_2=0.001$ μF [corresponding to the power spectra in Fig. 3(a)], while the open squares are for $C_1=0.1$ μF and $C_2=0.001$ μF [corresponding to the power spectra in Fig. 3(b)].

$$\frac{dx_5^r}{dt}=-\frac{1}{RC_2}[-x_4^r+0.11x_5^r+b_5(x_t-x_r)], \tag{2f}$$

$$\frac{dx_6^r}{dt}=-\frac{1}{RC_2}[-g(x_4^r)+x_6^r+b_6(x_t-x_r)], \tag{2g}$$

where the superscript *d* refers to the drive circuit and *r* refers to the response circuit. Note that the error signal x_t-x_r is fed back only into the high frequency part of the circuit, x_4 to x_6.

The parameters k_i and b_i are set to minimize the largest Lyapunov exponent for the response circuit corresponding to Eq. (2) [26,27]. The k_i's and b_i's are varied by a linear optimization routine in order to minimize the largest Lyapunov exponent for the response circuit. For the parameters listed in Table I, the largest Lyapunov exponent for the response circuit was -1160 s^{-1} (when $C_1=0.01$ μF and $C_2=0.001$ μF). There are many other possible combinations of the *k*'s and *b*'s that give similar Lyapunov exponents.

NOISE EFFECTS

The most interesting feature of this circuit is that by varying the ratio between C_1 and C_2 (varying the ratio between the frequencies of the two parts of the circuit), the amount of synchronization error caused by noise could be varied. To test this feature, white noise was added to the transmitted signal x_t [defined in Eq. (2a)]. The signal to noise ratio (S/N) was calculated by dividing the rms amplitude of x_t by the rms amplitude of the white noise. The synchronization error for the low frequency part of the circuit, $\delta(x_1)$, was calculated by dividing the rms amplitude of $x_1^d-x_1^r$ by the rms amplitude of x_1^d, where the superscript *d* refers to the drive circuit and *r* refers to the response circuit.

Figure 4 shows the synchronization error as a function of S/N for two different ratios of C_1 and C_2. The closed circles show the synchronization error when $C_1=0.01$ μF and $C_2=0.001$ μF, so that the fast frequency in the circuit is 1110 Hz and the slow frequency is 111 Hz (corresponding to the power spectra of Fig. 2). The synchronization error at a S/N of 1 (0 dB) is about 0.07, climbing to about 0.14 at a S/N of 0.33 (-4.8 dB). The minimum synchronization error at high S/N is about 0.02 because of mismatch between the circuits.

Clearly, when the frequency difference between the main frequencies in the circuit is larger, the synchronization error is smaller (the synchronization error for the higher frequency x_4 signals in the circuit was larger than the synchronization for the low frequency signals). The circuit acts as its own filter, so that the noise which contaminates the transmitted signal x_t is averaged out by the x_1 to x_3 part of the circuit. The relative improvement in synchronization error will depend on the specific circuit as well as the ratio of high to low frequencies, but by increasing the frequency ratio it should be possible to make the synchronization error smaller.

Since analog chaotic circuits have a finite bandwidth, one would expect that even a simple circuit would filter out some white noise, resulting in improved synchronization. In order to determine how much of the synchronization improvement was due to the two-frequency circuit, a pair of piecewise linear Rossler (PLR) circuits [25] were synchronized by unidirectional coupling. The PLR circuit is essentially the same as the two-frequency circuit described in Eq. (1), except that only the x_4, x_5, and x_6 components are present. To avoid

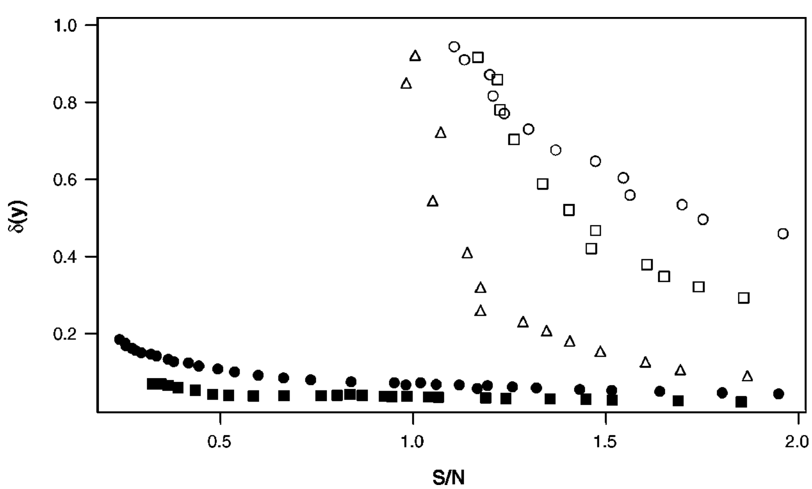

FIG. 5. rms synchronization error $\delta(y)$ from synchronized PLR circuits as a function of rms signal to noise ratio S/N. The open triangles are for $C=0.1$ μF, the open squares are for $C=0.01$ μF, and the open circles are for $C=0.001$ μF. The closed circles and squares are the data from Fig. 4.

confusion, these will be called y_1, y_2, and y_3. The circuit parameters were the same as for the fast part of the two-frequency circuit except that the capacitor C could be varied. The response was coupled to the drive circuit in the same fashion as for the two-frequency circuit [Eq. (2)], with the parameters $k_1=2.36$, $k_2=1.27$, $k_3=-1.12$, $b_1=-1.76$, and $b_2=b_3=0$.

Figure 5 shows the results of synchronizing the PLR circuits with noise added. The open triangles show the rms synchronization error as a function of S/N when $C=0.1\ \mu\mathrm{F}$ (the peak oscillation frequency for the PLR circuit was 11.1 Hz), the open squares are for $C=0.01\ \mu\mathrm{F}$ (peak frequency = 111 Hz), and the open circles are for $C=0.001\ \mu\mathrm{F}$ (peak frequency = 1110 Hz). The synchronization error was calculated from the y_1 signals. As the circuit frequency drops, so does its bandwidth, so the synchronization error will be smaller because more of the white noise is filtered out. The synchronization error still approaches 1 as the S/N approaches 1 for all of the PLR circuits, however, so the PLR circuit alone is not useful for $S/N<1$. Figure 5 also contains the data from Fig. 4 (closed circles and squares) as a comparison. Note that the synchronization error for the two-frequency circuit stays small even when $S/N<1$.

CONCLUSIONS

In previous synchronous chaotic circuits, there was a minimum S/N below which useful synchronization was not possible. In this two-frequency circuit, the synchronization error can always be made smaller by making the ratio between fast and slow frequencies larger. While increasing the frequency ratio would seem to increase the bandwidth of the transmitted signal, in practice this need not be true. Because there is a large separation between fast and slow frequencies, there is a large intermediate frequency region where there is no power in the chaotic signal. Simulations have shown that it is possible to filter out all but the frequencies near the two main peaks (using two bandpass filters with quality factors of $Q=1$) and still have stable synchronization. Before transmitting, the low frequency part of the chaotic signal may be mixed with an intermediate frequency sinusoidal signal to shift the chaotic signal up to any desired frequency range. The necessary bandwidth to synchronize the response circuit to the drive circuit is therefore only the bandwidth needed by the high frequency part of the signal. Increasing the ratio of high to low frequencies is equivalent to averaging the received signal over a longer time in order to average out noise.

[1] L. M. Pecora and T. L. Carroll, Phys. Rev. Lett. **64**, 821 (1990).
[2] T. L. Carroll and L. M. Pecora, IEEE Trans. Circuits Syst. **38**, 453 (1991).
[3] K. M. Cuomo, A. V. Oppenheim, and S. H. Strogatz, IEEE Trans. Circuits Syst., I: Fundam. Theory Appl. **40**, 626 (1993).
[4] H. Dedieu, M. P. Kennedy, and M. Hasler, IEEE Trans. Circuits Syst., I: Fundam. Theory Appl. **40**, 634 (1993).
[5] T. L. Carroll and L. M. Pecora, Physica D **67**, 126 (1993).
[6] L. Kocarev, K. S. Halle, K. Eckert, L. O. Chua, and U. Parlitz, Int. J. Bifurcation Chaos Appl. Sci. Eng. **2**, 709 (1992).
[7] G. Kolumban, M. P. Kennedy, and L. O. Chua, IEEE Trans. Circuits Syst., I: Fundam. Theory Appl. **44**, 927 (1997).
[8] K. Murali and M. Lakshmanan, Phys. Rev. E **48**, 1624 (1993).
[9] U. Parlitz, L. Kocarev, T. Stojanovski, and H. Preckel, Phys. Rev. E **53**, 4351 (1996).
[10] N. F. Rul'kov, A. R. Volkovski, A. Rodriguez-Lozano, E. Del-Rio, and M. G. Velarde, Chaos, Solitons Fractals **4**, 201 (1994).
[11] L. S. Tsimring and M. M. Sushchick, Phys. Lett. A **213**, 155 (1996).
[12] R. Brown, N. F. Rulkov, and N. B. Tufillaro, Phys. Rev. E **50**, 4488 (1994).
[13] E. J. Kostelich and J. A. Yorke, Phys. Rev. A **38**, 1649 (1988).
[14] R. Cawley and G. H. Hsu, Phys. Rev. A **46**, 3057 (1992).
[15] E. Rosa, S. Hayes, and C. Grebogi, Phys. Rev. Lett. **78**, 1247 (1997).
[16] T. Sauer, Physica D **58**, 193 (1992).
[17] T. L. Carroll, Phys. Rev. E **59**, 1615 (1999).
[18] T. L. Carroll, Phys. Rev. E **50**, 2580 (1994).
[19] T. L. Carroll, IEEE Trans. Circuits Syst., I: Fundam. Theory Appl. **42**, 105 (1995).
[20] N. F. Rulkov and L. Tsimring, Int. J. Circuit Theory Appl. **27**, 555 (1999).
[21] G. Gibson and C. Jeffries, Phys. Rev. A **29**, 811 (1984).
[22] X. Y. Zhang and H. Suhl, Phys. Rev. A **32**, 2530 (1985).
[23] S. M. Rezende, O. F. d. A. Bonfim and F. M. d. Aguiar, Phys. Rev. B **33**, 5153 (1986).
[24] T. L. Carroll, L. M. Pecora, and F. J. Rachford, Phys. Rev. A **40**, 377 (1989).
[25] T. L. Carroll, Am. J. Phys. **63**, 377 (1995).
[26] J. H. Peng, E. J. Ding, M. Ding, and W. Yang, Phys. Rev. Lett. **76**, 904 (1996).
[27] G. A. Johnson, D. J. Mar, T. L. Carroll, and L. M. Pecora, Phys. Rev. Lett. **80**, 3956 (1998).